

Conditional Generative Adversarial Network Aided High-Frequency Core Loss Predictions

Xiaobing Shen, Qingcheng Sui, Jiaze Kong, and Wilmar Martinez

Abstract—This report addresses the intricate task of estimating magnetic iron losses in high-frequency (HF) magnetic components through an innovative approach, employing a newly developed Conditional Generative Adversarial Network (cGANET) model. Moving away from conventional loss estimation methods that often fail to consider the complex interactions among various factors, our cGANET model is meticulously engineered to integrate a wide array of elements such as material characteristics, shape discrepancies, and ambient factors. This advanced method is supported by the use of a specialized four-wire measurement apparatus, greatly enhancing the training dataset with its broad spectrum of measurements. In comparison to traditional Deep Neural Network (DNN) models, cGANET not only achieves quicker convergence but also excels in accuracy for predicting iron losses. This model's exceptional performance, especially in situations beyond the scope of the training data, highlights its robustness and flexibility. The improvements in predictive precision and operational efficiency mark a significant stride in the development and refinement of HF magnetic components.

Index Terms—High-Frequency Magnetic Cores, Volumetric Iron Losses, Conditional Generative Adversarial Network (cGANET), Deep Neural Network (DNN), Multi-layer perceptron (MLP)

I. INTRODUCTION

RECENT strides in modeling magnetic materials use analytical models to tackle multidimensional effects [1]–[3]. DNNs, Transfer Learning, and LSTM have been employed for data-driven research in HF magnetics [4]–[6].

Standard neural networks have limitations, particularly in predictions outside the training data range. To overcome this, we introduce a Generative Adversarial Network (GANET)-based model. GANETs have shown promise in various fields, including image generation and electromagnetics [7]–[10]. They can augment datasets, enhancing the robustness of predictive models.

Our GANET-based model aims to improve prediction accuracy, especially for operational points outside the training data.

This report contributes in the following ways:

- Prepares training data for the cGANET model.
- Validates a GANET-based model for training accuracy and extrapolation capabilities.
- Tests the model's generality on different materials and datasets.

II. PROPOSED GANET MODEL FOR IRON LOSS PREDICTIONS

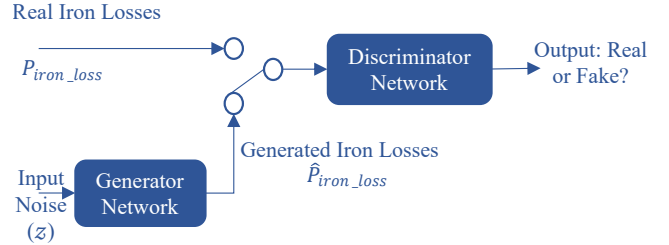


Fig. 1: Block Diagram of basic GANET

The GANET-based model surpasses the MLP model by enabling the creation of new data instances through innovative training techniques. Fig. 1 illustrates the GANET structure, consisting of the Generator, which synthesizes data akin to real instances, and the Discriminator, which discerns between real and synthetic data. The Generator's function is depicted as converting noise inputs (z) into data reflecting the desired distribution. The Discriminator's dual evaluation role is symbolized by a switch, underscoring its pivotal position in the GANET framework. The GANET training process is a strategic game where the Discriminator aims to accurately identify real data, counteracted by the Generator's attempts to produce increasingly convincing fakes. Fig. 2 introduces the Conditional GANET (cGANET), an evolution of the GANET model that incorporates a conditioning variable (x) into both Generator and Discriminator. Unlike standard GANETs that use single data points, cGANET employs pairs of input-output data ((x, y)), enriching the dataset and refining the training regime. The selection of cGANET for our predictive

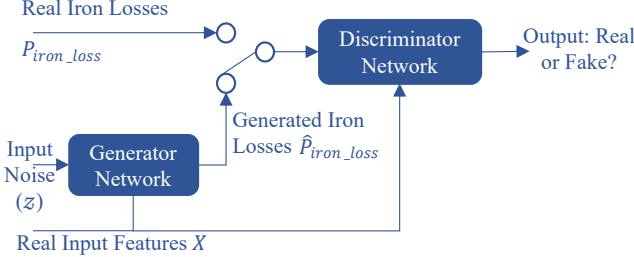


Fig. 2: Block Diagram of cGANET

modeling is due to its enhanced accuracy and context-awareness, essential for our application, as supported by [11].synthetic data.

A. Loss Functions of The Proposed GAN Model

A noise-injection architecture is used here. Within the framework of noise injection architecture, we introduce the noise denoted as z into the hidden layers at every level of the network. This mechanism is visually depicted in Fig. 3. It is worth noting that the dashed box, which signifies a concatenation block, is present in both Figure 3. The structure of the discriminator employed in our proposed model is depicted in Fig. 4. In a cGANET,

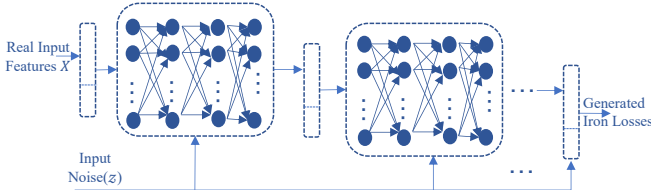


Fig. 3: Structure of The Noise-injection Generator

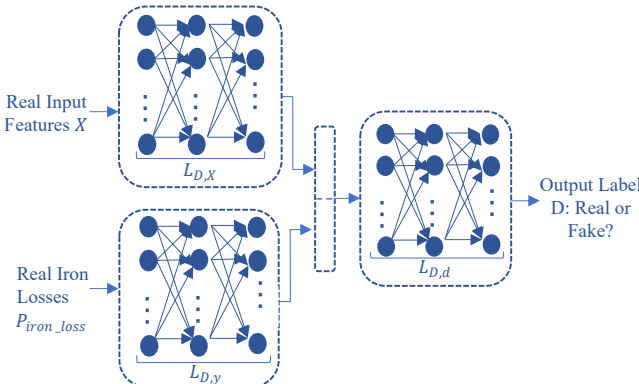


Fig. 4: Structure of The Noise-injection Discriminator

the generator and discriminator are conditioned on additional information such as class labels or data from other modalities. This additional information is provided

to both the generator and discriminator as input, which allows the cGANET to generate data that are conditioned on specific attributes.

The loss functions in a cGANET are modified to take into account the conditioning of the additional information. Here's a breakdown of the loss functions for both the discriminator and generator in a cGANET:

Discriminator Loss: The discriminator loss in a cGANET is similar to that of a traditional GANET, but with the condition information concatenated to the input. The loss is a sum of the losses for the real and generated (fake) data, and it's usually implemented as a binary cross-entropy loss. The discriminator wants to correctly classify real data as real and generated data as fake.

For a batch of data, the discriminator loss L_D can be formulated as [7]:

$$L_D = -\mathbb{E}_{\mathbf{x}, \mathbf{c} \sim p_{\text{data}}(\mathbf{x}, \mathbf{c})} [\log D(\mathbf{x}, \mathbf{c})] - \mathbb{E}_{\mathbf{z} \sim p_{\mathbf{z}}(\mathbf{z}), \mathbf{c} \sim p_{\text{data}}(\mathbf{c})} [\log(1 - D(G(\mathbf{z}, \mathbf{c}), \mathbf{c}))] \quad (1)$$

Where:

- D is the discriminator network.
- G is the generator network.
- \mathbf{x} is data sampled from the true data distribution $p_{\text{data}}(\mathbf{x})$.
- \mathbf{c} is the conditioning variable (like class labels).
- \mathbf{z} is the latent space vector sampled from distribution $p_{\mathbf{z}}(\mathbf{z})$ (typically a normal distribution).

Generator Loss: The generator's goal is to generate data that the discriminator will classify as real. In a cGANET, the generator is also conditioned on the additional information. The generator loss encourages the generator to create data that the discriminator will think is real [11].

The generator loss L_G can be expressed as:

$$L_G = -\mathbb{E}_{\mathbf{z} \sim p_{\mathbf{z}}(\mathbf{z}), \mathbf{c} \sim p_{\text{data}}(\mathbf{c})} [\log D(G(\mathbf{z}, \mathbf{c}), \mathbf{c})] \quad (2)$$

The generator tries to minimize this function. In practice, sometimes the generator loss is implemented as:

$$L'_G = \mathbb{E}_{\mathbf{z} \sim p_{\mathbf{z}}(\mathbf{z}), \mathbf{c} \sim p_{\text{data}}(\mathbf{c})} [\log(1 - D(G(\mathbf{z}, \mathbf{c}), \mathbf{c}))] \quad (3)$$

to provide stronger gradients during training, especially at the beginning when D is likely to reject samples from G with high confidence.

Overall Objective: The cGANET is trained by alternating between optimizing L_D and L_G (or L'_G). The complete min-max game between the generator and the discriminator can be summarized as follows:

$$\min_G \max_D L_{\text{cGANET}}(D, G) = L_D + L_G \quad (4)$$

(or $L_D + L'_G$ for the alternative generator loss).

This min-max game theoretically leads to a point where the generator produces perfect samples (indistinguishable from real data), and the discriminator is maximally confused, assigning a probability of 0.5 to both real and generated data. In practice, achieving this equilibrium is challenging and requires careful tuning of model architectures, learning rates, and other hyperparameters. At the beginning of the hyperparameters

TABLE I: Hyperparameters and Setups of cGANET-based Model

Hyperparameter	Value
Epochs	2000
Batch Size	32
Activation	ReLU
Performance	Relative Error
Learning Rate	Scheduler
Optimizer	Adam
Generator Parameters	118785 (464.00 KB)
Discriminator Parameters	99585 (389.00 KB)

tuning, some initial tests were applied to determine reasonable intervals for the hyperparameters. These initial setups consisted of shorter training runs with manually set parameters. The hyperparameters are set as in Table I. Then, the detailed structure of the hidden layers of the Generator and Discriminator were determined. The first two layers of the generator in Fig. 3 are with 128 nodes, connected to the following 4 layers with 64 nodes. For the Discriminator, $L_{(D,X)}$ and $L_{(D,y)}$ contain 2 layers with 64 nodes, followed by $L_{(D,d)}$ with 6 layers with 128 nodes in Fig. 4.

B. Results Analysis

Datasets from MagNet [12] are used to verify feasibility and generality, we use different training datasets from different materials. Four datasets, including Ferrites 3C90, 3C94, N87, and N49 from MagNet [12], were used to extend the evaluation of the proposed model. All the datasets were divided into two sets, one for the training process (75% of the whole set), and one beyond the former training set (the rest 25%) for the extra new test to verify its data augmentation and enhancement for predicting the scenarios beyond the training dataset.

For MagNet data, the input features include flux densities, frequencies, and temperature. The number of data items is smaller than that of our measurements, as shown in Table II. With limited data, the model still can work as a prediction model for totally new scenarios of one certain magnetic material. The training data range is 25 - 70°C, while the extra new test data is with 90°C, extending beyond the training set.

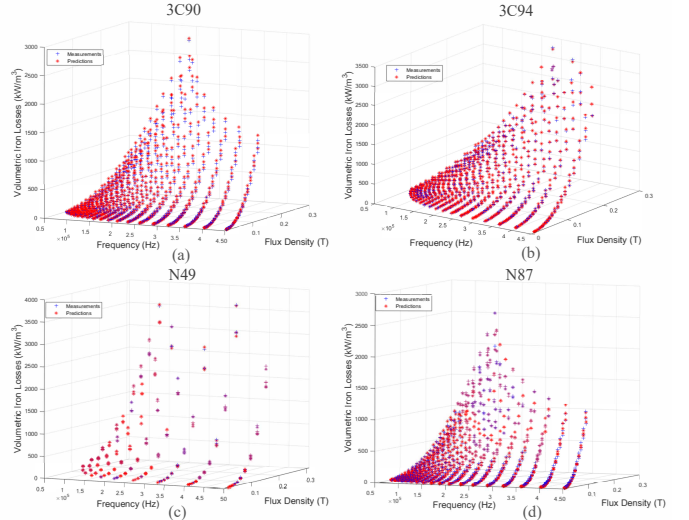


Fig. 5: Scatter Plot for Training Process of cGANET with: (a) 3C90, (b) 3C94, (c) N49, (d) N87 Datasets from MagNet

As the results of the cGANET model, Fig. 5 shows the scatter plot of predictions and measurements during the training process with these four datasets. N49 only has 249 data items for training, and it still can train the model well with an R-value of 0.9998. New datasets beyond the training data were applied after the proposed model was trained.

Fig. 6 shows scatter plots of predictions and measurements with new test data beyond the training set. All four materials can predict the unseen scenarios outside the range of the test data. All four plot results have R-values over 0.9900. The data augmentation and enhancement abilities are not affected by data sizes and sources. Table II presents the cGANET-based models in terms of training performance and new test experiments. This demonstrates cGANET's enhanced predictive ability in scenarios beyond the training range.

III. DATA PREPARATION FOR MAGNET CHALLENGE

The datasets encompass five provided materials, labeled as A, B, C, D, and E, each with a distinct count of data points in both training and testing phases.

The training dataset consists of five CSV files, featuring measurements for B_Field (in Teslas), H_Field (in Amps per meter), Frequency (in Hertz), Temperature (in degrees Celsius), and Volumetric_Loss (in Watts per cubic meter). The files follow a structure of $N \times 1024$ for B_Field and H_Field, and $N \times 1$ for Frequency, Temperature, and Volumetric_Loss, where N signifies the number of data points.

The distribution of data points for each material is as follows:

TABLE II: Overview of Datasets Used for Proposed cGANET-based Model

Materials	Source	Model	Data Items	R-value		Training Time (s)	Epoch
				Training	New Test		
3C90	MagNet	cGANET	1548	0.9997	0.9989	197.30	2000
3C94	MagNet	cGANET	1394	0.9998	0.9985	195.59	2000
N49	MagNet	cGANET	333	0.9998	0.9951	198.27	2000
N87	MagNet	cGANET	1603	0.9994	0.9972	198.55	2000

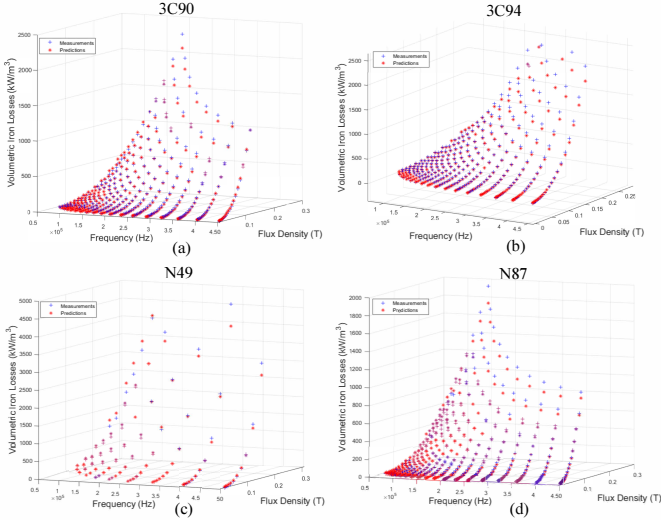


Fig. 6: Experimental Results of cGANET with New Data Tests of (a) 3C90, (b) 3C94, (c) N49, (d) N87 Datasets from MagNet

- Material A: 2432 data points for training, 7651 for testing.
- Material B: 7400 data points for training, 3172 for testing.
- Material C: 5357 data points for training, 5357 for testing.
- Material D: 580 data points for training, 7299 for testing.
- Material E: 2013 data points for training, 3738 for testing.

Our data preparation strategy can be conclude as follows:

- 1) **Waveform Categorization:** We classify different waveform shapes (sinusoidal, triangular, trapezoidal) as hot vectors, aiding in the analysis of waveform impact on magnetic properties.
- 2) **Feature Selection:** Our input features include flux density, frequency, and temperature, crucial in determining the magnetic behavior under different conditions.
- 3) **Target Value Identification:** The primary objective is to predict the volumetric core loss, our target

metric for assessing material efficiency.

- 4) **Data Normalization and Cleaning:** We normalize the data for comparability and clean it to address any inconsistencies or missing values.
- 5) **Feature Engineering:** We explore feature engineering techniques to potentially enhance model performance.

As part of our data preparation, we represent waveform types as hot vectors and include other parameters such as flux density, frequency, and temperature. Below is an example table showcasing the hot vector for waveforms. Our data preparation methodology is designed to

TABLE III: Example of Hot Vector Representation for Waveforms

Sinusoidal	Triangular	Trapezoidal
1	0	0
0	1	0
0	0	1

effectively handle the complexity and diversity of the provided datasets. By categorizing waveforms, selecting relevant features, and focusing on volumetric core loss prediction, we aim to develop robust models for accurate assessment of the magnetic properties of these materials under various conditions.

IV. RESULTS FOR MAGNET CHALLENGE DATA

After data preparation, the proposed cGANET model was trained with the provided five materials. The average relative error of the training process of each material can be found in Fig. 7.

The scatter plot with the R-value can be seen in Fig. 8. The results highly align with the results from Section II, which use the datasets from Magnet website with single excitation. Then our code is provided along with report, as well as the prediction for the test data.

The training process validates the use of cGANET for high-frequency magnetic core losses. And with the experiments in Section II confirm the prediction ability of the proposed cGANET model for the input beyond the training data range. Furthermore, with all the different materials and excitation waveforms, cGANET still holds

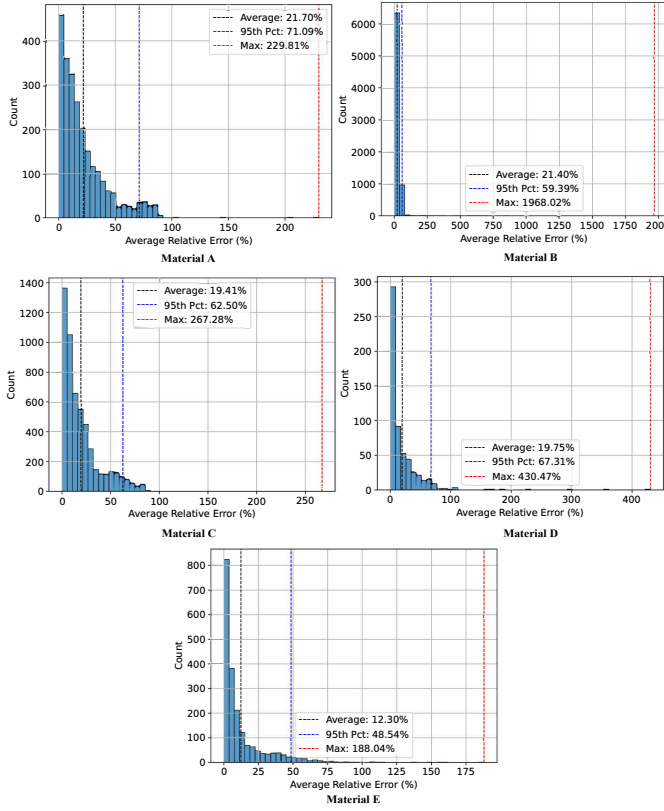


Fig. 7: Average Relative Errors of 5 Materials

the ability to provide accurate predictions. For Magnet Challenge, the flux density data doesn't have any noise ideally, which makes the training behavior a bit uglier, compared with the real data from the Magnet website. The concept of cGANETs applied to core loss prediction is appealing, providing accurate results on data for which the model has not been trained before. Besides, the impressive accuracy achieved even on sparse data, cGANETs effectively solve the problem associated with extrapolation on some conventional neural networks.

REFERENCES

- [1] N. Rasekh, J. Wang, and X. Yuan, "Artificial neural network aided loss maps for inductors and transformers," *IEEE Open Journal of Power Electronics*, vol. 3, pp. 886–898, 2022.
- [2] H. Li, S. R. Lee, M. Luo, C. R. Sullivan, Y. Chen, and M. Chen, "Magnet: A machine learning framework for magnetic core loss modeling," in *2020 IEEE 21st Workshop on Control and Modeling for Power Electronics*, 2020, pp. 1–8.
- [3] E. Dogariu, H. Li, D. S. López, S. Wang, M. Luo, and M. Chen, "Transfer learning methods for magnetic core loss modeling," in *2021 IEEE 22nd Workshop on Control and Modelling of Power Electronics (COMPEL)*, pp. 1–6.
- [4] H. Li, D. Serrano, T. Guillod, E. Dogariu, A. Nadler, S. Wang, M. Luo, V. Bansal, Y. Chen, C. R. Sullivan, et al., "Magnet: An open-source database for data-driven magnetic core loss modeling," in *2022 IEEE Applied Power Electronics Conference and Exposition (APEC)*. IEEE, 2022, pp. 588–595.
- [5] D. Serrano, H. Li, S. Wang, T. Guillod, M. Luo, V. Bansal, N. K. Jha, Y. Chen, C. R. Sullivan, and M. Chen, "Why magnet: Quantifying the complexity of modeling power magnetic material characteristics," *IEEE Transactions on Power Electronics*, vol. 38, no. 11, pp. 14 292–14 316, 2023.
- [6] R. Y. M. Li, B. Tang, and K. W. Chau, "Sustainable construction safety knowledge sharing: A partial least square-structural equation modeling and a feedforward neural network approach," *Sustainability*, vol. 11, no. 20, p. 5831, 2019.
- [7] A. Creswell, T. White, V. Dumoulin, K. Arulkumaran, B. Sen-gupta, and A. A. Bharath, "Generative adversarial networks: An overview," *IEEE signal processing magazine*, 2018.
- [8] Z. Qin, Z. Liu, P. Zhu, and W. Ling, "Style transfer in conditional gans for cross-modality synthesis of brain magnetic resonance images," *Computers in Biology and Medicine*, 2022.
- [9] O. Noakosteen, J. Vijayamohan, A. Gupta, and C. Christodoulou, "Antenna design using a gan-based synthetic data generation approach," *IEEE Open Journal of Antennas and Propagation*, vol. 3, pp. 488–494, 2022.
- [10] M. Baldan and P. Di Barba, "Discovering pareto-optimal magnetic-design solutions via a generative adversarial network," *IEEE Transactions on Magnetics*, vol. 58, no. 9, 2022.
- [11] J. Oskarsson, "Probabilistic regression using conditional generative adversarial networks," 2020.
- [12] Princeton-Dartmouth-Plexim MagNet Project, "Data-driven methods for power magnetics modeling," accessed: Jul. 8, 2023. [Online]. Available: <https://mag-net.princeton.edu/>

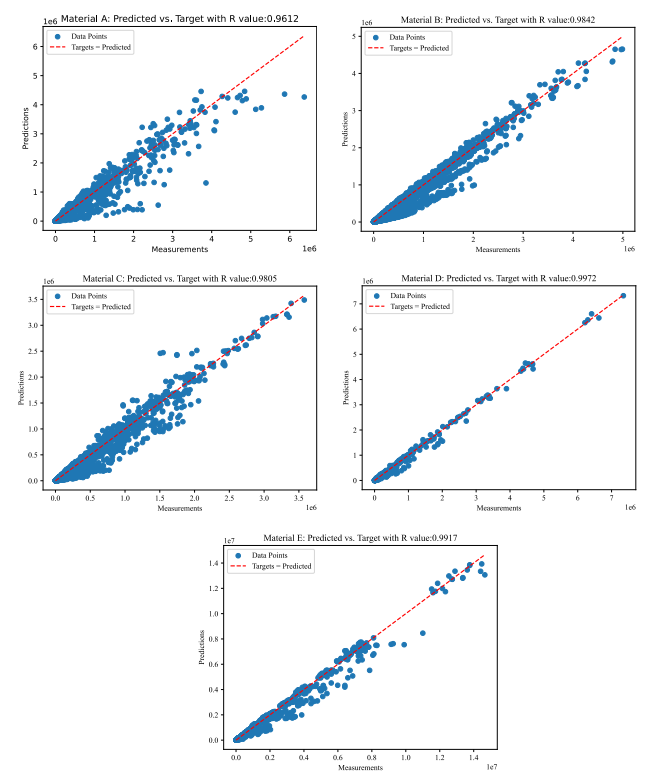


Fig. 8: Experimental Results of cGANET with 5 Materials from MagNet Challenge